ELSEVIER

Coordination Chemistry Reviews
148 (1996) 183–197

COORDINATION CHEMISTRY REVIEWS

Supramolecular structure in extramembraneous antennae of green photosynthetic bacteria

Hitoshi Tamiaki

Department of Bioscience and Biotechnology, Faculty of Science and Engineering, Ritsumeikan University, Kusatsu, Shiga 525-77, Japan

Received 1 February 1995; in revised form 10 June 1995

Contents

Abstract

Supramolecular structures in extramembraneous antennae of green photosynthetic bacteria (so-called "chlorosomes") are reviewed. In chlorosomes, bacteriochlorophylls-*c*, *d* and *e* (magnesium complexes of chlorins with a 1-hydroxyethyl group) self-aggregate to form the main light-harvesting components. This arrangement is unique and different from that in other antennae where the pigments bond with some proteins. Model studies of artificial aggregates and comparison of in-vitro aggregates with in-vivo aggregates provide useful insights in the elucidation of the supramolecular structures. The pigments in natural chlorosomes self-aggregate with the assistance of a special hydrogen-bond, C=O···H(X)O···Mg and π–π interaction of the cyclic tetrapyrroles. Magnesium chlorins thus form a two-dimensional sheet and subsequent rolling of the sheet makes a rod of the main components in chlorosomes.

Keywords: Extramembraneous antennae; Chlorosomes; Supramolecular structures; Photosynthetic bacteria; Self-aggregates; Bacteriochlorophylls

SSDI 0010-8545(95)01188-9

1. Introduction

Photosynthetic bacteria are divided into three types: purple, green and heliobacteria. The green bacteria can be further divided into two families, *Chlorobiaceae* and *Chloroflexaceae* [1,2]. Green photosynthetic bacteria have two types of light-harvesting antennae, intramembraneous and extramembraneous antennae. The extramembraneous antennae are referred to as "chlorosomes", and are located on the inner surface of the cytoplasmic membrane containing the intramembraneous antennae and the reaction center. The chlorosomes are unique antenna systems and have an egg-like ellipsoidal form with the dimensions of 106 nm × 32 nm × 12 nm for *Chloroflexus aurantiacus*, one of the *Chloroflexaceae*. In the chlorosomes, a lipid monolayer surrounds oligomers of several rod elements which are the main components for light absorption. The pigments have absorption maxima at 640–670 nm in the in-vitro monomer and maxima at 720–760 nm in the chlorosomal rod [3]. The red shift in vivo indicates that the rods are built-up by aggregation of the pigment molecules. These main pigments are magnesium complexes of chlorin (a cyclic tetrapyrrole) with hydroxy and oxo groups at the 3^1- and 13^1-positions, respectively. In spite of the chlorin chromophore, the compounds are named bacteriochlorophyll(=BChl)-*c*, *d* and *e* because they were found in green bacteria. Evidently, BChls-*c*, *d*, *e* have a chlorin π-system (17,18-dihydroporphyrin) but not a bacteriochlorin chromophore (7,8,17,18-tetrahydroporphyrin), which is seen in BChls-*a* and *b*. BChls-*c*, *d*, *e* indicate a family of molecules with a variety of aliphatic substituents at the R^8, R^{12}, and R positions as shown in Fig. 1 [4]. In *Chloroflexus aurantiacus*, for example, BChl-*c* is composed of a mixture of several molecules; R^8 = Et, R^{12} = Me, R = $C_{16}H_{33}$, $C_{18}H_{35,37}$, $C_{20}H_{33,39}$ with $R/S = 2/1$ at the 3^1-chiral center [5].

How the pigments make the rod elements in the chlorosomes has attracted much attention. From comparison with other well-defined antennae, it had been believed that BChls-*c*, *d*, *e* bonded with α-helical peptides to form the aggregates [2,6]. On

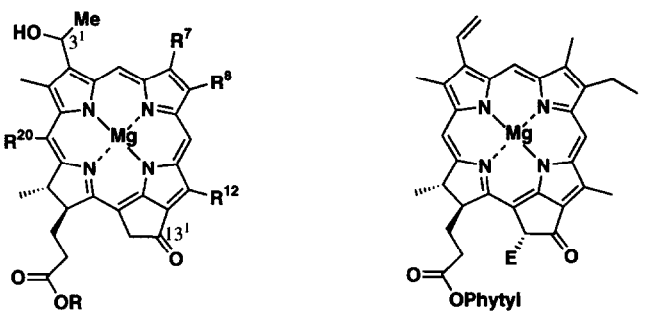

BChl-*c*: R^7 = R^{20} = Me
BChl-*d*: R^7 = Me, R^{20} = H
BChl-*e*: R^7 = CHO, R^{20} = Me
(R^8, R^{12} = alkyl groups, R = a long chain)

Chl-*a*: E = COOMe
pyroChl-*a*: E = H

Fig. 1. Structures of magnesium chlorins.

the other hand, Bystrova et al. [7] first proposed that such a peptide might be unnecessary for in-vivo aggregation because BChl-*c* easily self-aggregates in non-polar organic solvents. Griebenow et al. [8–15] showed by visible, circular dichroism (CD), linear dichroism (LD) and resonance Raman (RR) spectra that the native chlorosomes (*Chloroflexus aurantiacus*) are similar to protein-free chlorosomes prepared by gel-electrophoretic filtration. They also first confirmed experimentally the self-aggregation of BChl-*c* in natural chlorosomes. Hirota et al. [16] and other groups [17–19] supported the in-vivo self-aggregation by reconstruction experiments of chlorosomes. Recently, many researchers have accepted that the in-vivo aggregates are a result of self-aggregation rather than specific interaction of BChl-*c* and *d* with polypeptides. However Niedermeier et al. [20] and Lehmann et al. [21,22] have still argued for the interaction of pigments with peptides in chlorosomes from the visible and CD spectra.

The supramolecular structure of the chlorosomal aggregates has still not been determined, nor the functions of the aggregates in the ultra-fast and highly efficient energy migration in the chlorosomes and selective energy transfer to other components (finally to the reaction center) [14,15,23–29]. Here, I will review the studies of supramolecular structures for chlorosomes, including our recent model studies, and propose a supramolecular structure formed by self-aggregation of BChl-*c* and *d* as the most probable structure for the in-vivo chlorosomes.

2. Supramolecular structure of self-aggregates

2.1. In-vitro BChl-c aggregates

2.1.1. Model (A) (see Fig. 2)

Bystrova et al. [7] first reported self-aggregation of BChl-*c* in non-polar organic solvents and solid films in 1979. They observed the red shift of visible absorption bands of BChl-*c* in carbon tetrachloride–heptane (1:9) and in solid films prepared by evaporation of the ether solution (typically 662 (ether solution) to 745 nm shifting of the Q_y band). This red shift band was observed in the presence and absence of water, which was necessary for the formation of such a band in aggregates of chlorophyll(=Chl)-*a*. They claimed self-aggregation of BChl-*c*. Bacteriopheophytin(=BPhe)-*c* (without magnesium as the central metal) gave no red shift in non-polar organic solvents, thus determining that magnesium was necessary for self-aggregation. The infrared (IR) spectra of the self-aggregates were measured, giving the following bands; 1741, 1650, 1610 (solution) and 1737, 1650, 1607 cm^{-1} (film). The first band (1737–1741 cm^{-1}) was unambiguously assigned to ester carbonyl stretching band free from any interaction. The second peak (1650 cm^{-1}) was assigned to 13^1-keto carbonyl coordinating to magnesium by comparing with reported IR data of several magnesium chlorins [34]. In the film, a 3180 cm^{-1} peak was observed which was assigned to 3^1-hydroxyl stretching with some interaction, presumably coordination to magnesium. As a result, model (A) was proposed as self-aggregates of BChl-*c*; six-coordinated magnesium with oxygens of the keto carbonyl

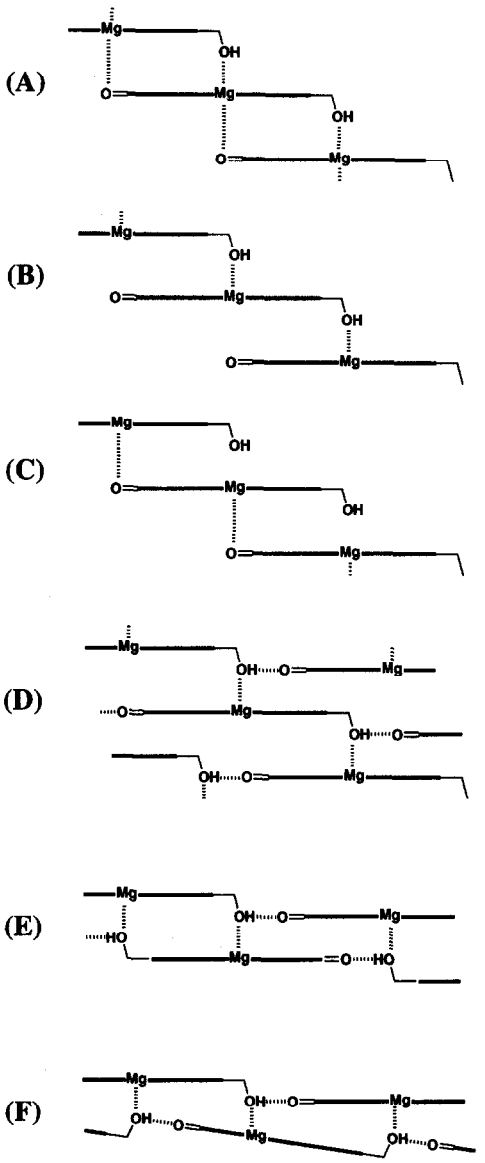

Fig. 2. Proposed schematic models for BChl-*c* self-aggregates.

and hydroxyl groups as axial ligands (see Fig. 2). Olson et al. [35] measured visible and CD spectra of BChl-*c* aggregates. These spectra were simulated by calculation using a point-dipole approximation method. They claimed that about 10 BChl-*c* molecules aggregated to form a helical arrangement by use of model (A). From visible, CD, IR and RR spectra of aggregates of BChl-*c* extracted from *Chloroflexus*

aurantiacus, Blankenship et al. [36,37] revised the model (A) as having asymmetric six-coordinated magnesium atoms out of the chlorin π-plane.

Recent results show that the electronic and vibrational absorption data by Bystrova et al. are correct but the interpretation was incorrect (see Section 2.3). In particular, wrong assignment of the 1650 cm^{-1} peak to C=O···Mg led to the erroneous proposal of model (A).

2.1.2. Model (B)

Smith et al. [38] measured visible spectra of BChl-*c* and *d* and also zinc analogues (with zinc as the central metal instead of magnesium) in dichloromethane–hexane (1:200). The addition of methanol resulted in the 748 nm peak in the spectra of BChl-*c* shifting to 662 nm. Compounds with a vinyl or an ethyl group at the 3-position instead of the 1-hydroxyethyl group, as well as those without magnesium or zinc as the central metal, gave no absorption bands at longer wavelengths (>700 nm) characteristic of aggregates. On the other hand, the molecule with a 13^1-hydroxyl group prepared by reduction of the 13^1-ketone showed similar absorption bands to the molecule with the intact keto group, indicating the presence of aggregates. Therefore, they claimed the contribution of the magnesium and 3-(1-hydroxyethyl) substituents in the aggregation was necessary and the 13^1-keto carbonyl substituent was less important. Thus model (B) was proposed; five-coordinated magnesium with the hydroxyl group as an axial ligand.

In the model (B), the 13^1-keto carbonyl group is free from any interaction, which is inconsistent with IR data in Section 2.1.1. The reason for this misrepresentation is discussed in Section 2.2.

2.1.3. Model (C)

Lutz et al. [39,40] measured the RR spectra of a 1 mM dry carbon tetrachloride solution of BChl-*c* (*Chlorobium limicola*) at 20 K. The peaks, 1639, 1609, 1584, 1554 cm^{-1} were observed in the region of 1500–1750 cm^{-1}. The last three peaks were due to the C–C and C–N stretching of chlorin chromophore, clearly indicating the presence of 5-coordinated magnesium in the aggregates. The 1639 cm^{-1} peak was due to 13^1-keto carbonyl stretching which was about 50 cm^{-1} down-shifted compared with 1685–1690 cm^{-1} peaks observed from monomeric BChl-*c* in pyridine or THF. When BChl-*c* was dissolved in a secondary alcohol, the stretching of the C=O hydrogen-bonded with the alcoholic solvent was observed at least at 1655 cm^{-1}. The 1639 cm^{-1} peaks were so small that the peaks were assigned to the stretching of 13^1-C=O coordinating to magnesium. As a result model (C) was proposed; five-coordinated magnesium with the carbonyl group as an axial ligand.

If the model (C) is true, the compounds without a 3^1-hydroxyl group would form aggregates, which is inconsistent with visible data in Section 2.1.2. As mentioned in 2.1.1, the wrong assignment of 1639 cm^{-1} peak to C=O···Mg mistakenly led to the model (C). A solvent alcoholic hydroxyl group is different from the OH coordinating to magnesium. This point is discussed in Section 2.2.

2.1.4. Model (D)

Worcester et al. [41] studied small-angle neutron scattering of chlorophyll micelles. BChl-*c* in dry deuterated toluene–deuterated octane (1 : 1) made about 11 nm diameter cylindrical micelles with a 750 nm absorption band. A two-dimensional lattice model (D) with hydrogen bonding between the free hydrogen atom of the magnesium-coordinated hydroxyl group and the keto C=O functions in another chain was considered.

The model (D) is discussed in Sections 2.2 and 2.3.

2.1.5. Models (E) and (F)

Brune et al. [42] measured visible and IR spectra of BChl-*c* (from *Chloroflexus aurantiacus*) in dry carbon tetrachloride. A visible band at 740 nm and an IR band at 1650 cm^{-1} were observed in concentrated carbon tetrachloride solution of BChl-*c*, whereas addition of 0.1% pyridine to the solution shifted the bands to 670 nm and 1687 cm^{-1}. The magnesium chlorin with a vinyl group at the 3-position, called pyrochlorophyll(= pyroChl)-*a*, showed a band at 680 nm in heptane and 1654 cm^{-1} frequency in hexane. These results showed the necessity of the 3^1-OH group for aggregation and the 13^1-C=O stretching in C=O···Mg at 1654 cm^{-1}, not 1650 cm^{-1}. They accepted the presence of 5-coordinated magnesium from reported RR results (see 2.1.3) and claimed the contribution of Mg, OH and C=O in the formation of BChl-*c* aggregates from their own results. In contrast with the assignment by Bystrova et al. (see 2.1.1), the 1650 cm^{-1} band was ascribed to the C=O stretching in C=O···HO···Mg in consideration with several previous reports (see a review by Katz et al. [43] for how the assignment varied). They considered the presence of C=O···H(X)O···Mg in the aggregates and proposed an anti-parallel chain model (E) and a stepped, parallel chain model (F).

Uehara et al. [44,45] measured the visible and IR spectra of BChl-*c* from *Chlorobium limicola* in water-saturated carbon tetrachloride. A concentrated aqueous carbon tetrachloride solution of BChl-*c* with R^8 = ^{i}Bu, R^{12} = Me or Et and R = farnesyl gave exclusively aggregates with a 747 nm absorption band and a 1641 cm^{-1} vibration band. The 1641 cm^{-1} band was due to 13^1-carbonyl stretching in C=O···H(X)O···Mg (vide supra). With increasing concentration of BChl-*c*, visible absorption bands were shifted to longer wavelength and deconvolution of the visible spectra might reveal the successive shift from monomer to tetramer through dimer and finally to polymer formed by 20–40 molecules. They claimed support for model (F) from the IR results that the dimer and tetramer structures should be depicted in a parallel orientation (head-to-tail type, vide infra). Alden et al. [46] simulated the visible absorption and fluorescence data of the aggregates by calculation using exciton models, which supported model (F).

Nozawa et al. [47–49] measured ^{13}C NMR spectra of the BChl-*c* aggregate solids. The intermolecular distance between $C13^1$ and $C3^1$ was estimated to be similar to the intramolecular distance between C20 and $C3^1$ (four bonds apart) by means of rotational resonance cross polarization–magic angle spinning spectroscopy. They also ascribed the dimeric structure of BChl-*c* in $CDCl_3$ to an anti-parallel head-to-head dimer (vide infra) by ^{1}H NMR spectroscopy [50]. The visible spectra in

dichloromethane–hexane showed gradual change from monomer to large aggregates through dimer and small aggregates [51]. They supported the model (E) which consisted of aggregation of the head-to-head dimer. Theoretical analysis of the visible absorption spectral shift should indicate the stacking of the anti-parallel chains (model (E)) in the aggregates.

The analysis of the visible, IR and NMR data led to the models (E) and (F) for the in-vitro BChl-*c* aggregates. From the above experiments, it is still unclear whether the structurally well-defined dimers directly give the aggregates, i.e., the dimers form a part of the aggregates. This point is discussed in Section 2.2. Moreover, the models (E) and (F) are possible in the in-vitro aggregates prepared under the each conditions. It is discussed in Section 2.3 whether these models are adequate or not to describe the supramolecular structure of the in-vivo BChl-*c* aggregates.

2.2. *Aggregates of synthetic zinc chlorins as BChl-c models*

BChl-*c* is a magnesium complex and easily demetallates to give BPhe-*c* even under weak acidic conditions. BChl-*c* has a 1-hydroxyethyl group in the molecule and often dehydrates to give the corresponding vinyl analogue. The 1-hydroxyethyl substituent affords a chiral center at the 3^1-carbon and racemization can occur to give diastereomeric mixtures. To overcome these problems, a zinc chlorin **1** with a hydroxymethyl group at the 3-position was synthesized (see Fig. 3) [30]. This compound was more stable under acidic and basic conditions than BChl-*c*. The zinc chlorin was readily available owing to the use of Chl-*a* as the starting material, which was obtained by extraction from commercially available algae.

The model zinc compound **1** dissolved in dichloromethane with a small amount of a polar reagent (tetrahydrofuran or methanol) showed several peaks in the visible region (λ_{max} (Soret) = 426 and (Q_y) = 652 nm), which were characteristic of monomeric form. When the solution was diluted with hexane, new bands (λ_{max} (Soret) = 450 and (Q_y) = 740 nm) appeared while concomitantly the monomeric peaks decreased. The predominant bands growing in the non-polar solvents had three characteristic points compared with the monomeric absorption; (i) broad, (ii) red-shifted, and (iii) low ratio in the Soret/Q_y absorbance. Such a spectrum is attributed to *J*-aggregation of the model molecules. Addition of larger amounts of methanol (> 5% (v/v)) or highly coordinatable pyridine (> 0.1% (v/v)) changed the absorption spectrum to the monomeric one, in which the peaks were sharp and the λ_{max} were blue-shifted.

The visible absorption spectrum of the artificial aggregate of **1** in non-polar solvents was very similar to that of the in-vivo aggregates of BChl-*c* in natural chlorosomes as well as to that of the in-vitro aggregates of BChl-*c* in non-polar organic solvents. In particular, the red shifts of the Q_y band of **1** and BChl-*c* from the monomer to the aggregate were about 1800 and 1600–1800 cm^{-1}, respectively (Table 1). Obviously, the supramolecular architecture of the artificial aggregate of **1** in non-polar organic solvents may very well serve as a model for the organization of self-aggregates of BChl-*c*.

To determine the chromophores necessary for such aggregation, visible spectra of several compounds **2**–**4** (see Fig. 3) were measured [30]. Compound **2** (without

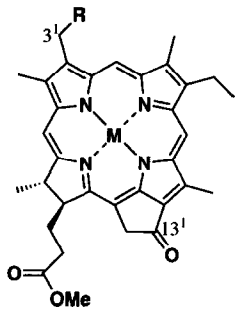

1 : M = Zn, R = OH
2 : M = H_2, R = OH
3 : M = Zn, R = Me
8 : M = Zn, R = NMe_2
9 : M = Zn, R = NHMe
10 : M = Zn, R = NH_2
11 : M = Mg, R = Me
13 : M = Mg, R = OH

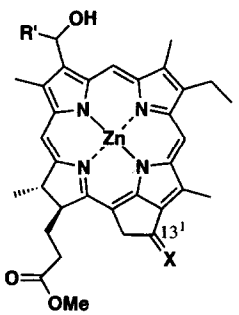

4 : R' = H, X = H_2
5 : R' = Me, X = H, OH
6 : R' = Me, X = O

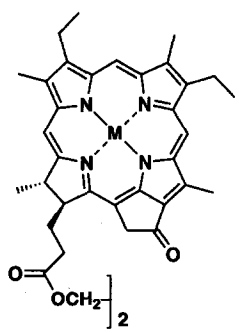

7 : M = Zn
12 : M = Mg

Fig. 3. Structures of model compounds.

central zinc) in dichloromethane gave a monomeric spectrum and in dichloromethane–hexane (1:99) gave less-shifted bands, where the compound was still monomeric. With compound **3** (without a 3^1-hydroxyl group), little change was observed in the visible region of the spectra on decreasing the solvent polarity. Compound **4** (without a 13^1-keto carbonyl group) in dichloromethane–hexane (1:99) showed mainly a monomeric absorption band with a small shoulder on the red side of the Soret and Q_y bands. The shoulders are probably due to dimer formed by mutual coordination of a hydroxyl group in one molecule to a zinc in another molecule; an anti-parallel head-to-head dimer (vide infra). These results indicate that central zinc,

Table 1
Red shift $\Delta\lambda$ of Qy absorption band by aggregation of various metallochlorins

Compound	λ_{max} (nm)		$\Delta\lambda$ (cm^{-1})	Structure	Ref.
	monomer	aggregate			
Zn–**1**	652	740	1820	Fig. 3	30
Mg–**13**	658	755	1950	Fig. 3	31
BChl-*c* (in vitro)	660	740	1640	Fig. 1[a]	15
BChl-*c* (in vivo)	660	740	1640	Fig. 1[a]	15
BChl-*c* (in vitro)	662	748	1740	Fig. 1[b]	38
BChl-*c* (in vivo)	662	750	1770	Fig. 1[b]	38

[a] R^8 = Et, R^{12} = Me. [b] R^8 = Et, ^{n}Pr, or ^{i}Bu, R^{12} = Me or Et.

3^1-hydroxyl and 13^1-keto carbonyl groups are necessary for aggregation and that these three sites are coordinated to each other in the aggregate. Smith et al. [38] have already reported (see 2.1.2) that a 13^1-keto carbonyl group was not necessary for aggregation in non-polar organic solvents because the compounds **5** and **6** showed similar red shift of visible peaks. The 13^1-*dihydro*-compound **4** showed little red shift in non-polar solvents and the oxygen at the 13^1-hydroxyl group of **5** should induce aggregation similarly to that of the 13^1-keto carbonyl group of **6**.

Zinc complexes with a cyclic tetrapyrrole ligand (H_2N_4; porphyrin, chlorin, etc.) could take 4- or 5-coordinated states but not a 6-coordinated state [52]; zinc chlorins take no axial ligand to be square planar ZnN_4 or one axial ligand (L) to be pyramidal ZnN_4L but do not take two axial ligands as shown in ZnN_4L_2. Titration experiments showed that a methanol molecule coordinated to the central zinc of **3** more strongly than an acetone molecule by use of visible absorption spectroscopy. In the aggregates, the 3^1-hydroxyl group coordinates to the zinc exclusively to form a 5-coordinated ZnN_4O which could have no more axial ligands. The third component for aggregation, the 13^1-keto carbonyl group, hydrogen-bonds with a 3^1-hydroxyl group. Therefore, zinc–**1** aggregates are formed by coordination of the 3^1–hydroxyl group of one molecule with the central zinc of another molecule and successive special hydrogen-bonding of the coordinating hydroxyl group with the 13^1-keto carbonyl group of a third molecule, C=O···H(X)O···Zn.

To confirm the bonding skeleton in the aggregates, RR spectra of model compounds were measured in solution at room temperature [53]. Excitation at 413 nm of zinc chlorin **3** with an ethyl group at the 3-position in dichloromethane–hexane (1:99) gave RR peaks at 1705, 1624, 1568, 1545 cm^{-1} (see Table 2). The 1705 cm^{-1} band comes from the carbonyl stretching vibration of the 13^1-keto group. Such a high frequency shows that the keto group is free from any intermolecular interaction. Several bands below 1630 cm^{-1} show that the central zinc is 4-coordinated without axial ligands. The zinc–**3** in the solvents must be monomeric as shown in the visible spectrum (vide supra).

Visible spectral analysis of compound **7** in dichloromethane, with two zinc–chlorin chromophores (see Fig. 3) indicated that the zinc–chlorin moieties hardly interacted

Table 2
Resonance Raman shift of metallochlorins in non-polar organic solvents

Compound	ν_{max} (cm^{-1})						Comments
Zn–**3**	1705		1624		1568	1545	monomer
Zn_2–**7**		1654	1620		1562	1540	methanol-assisted dimer
Zn–**1′**	1701	1651	1620		1560	1540(sh)	monomer + aggregate
Mg–**11**	1698		1612	1584	≈1550	≈1530	monomer
Mg_2–**12**		1646	1614	1590	≈1550	≈1525	methanol-assisted dimer
Mg–**13**	1694	1642	1611	–	≈1550	≈1530	monomer + aggregate

with each other. After dilution of the solution with 100-times volume of hexane and successive addition of a small amount of methanol (0.01% (v/v)), the Q_y band in the visible spectrum was red-shifted by about 700 cm^{-1} [53], indicating the formation of a methanol-assisted complex reported by Boxer et al. [54] (see Fig. 4). In the complex, the 13^1-C=O stretching vibration was measured at 1654 cm^{-1}. Addition of methanol-d_4, instead of methanol, changed only the carbonyl peak, shifting it about -1 cm^{-1}. The carbonyl of **7** interacted with hydrogen of the hydroxyl group of the added methanol. The chlorin C–C and C–N stretching peaks of dimeric **7** (1500–1630 cm^{-1}) were shifted lower in frequency than those of monomeric **3**. This implies that the central zinc of **7** was 5-coordinated with one axial ligand. Therefore, the RR spectra of **7** also showed that **7** makes the methanol-assisted complex, as expected from the visible absorption spectra. The 1654 cm^{-1} band is clearly assigned to the 13^1-keto carbonyl stretching vibration C=O···H(Me)O···Zn.

The visible spectrum of zinc chlorin **1′** (=stearyl ester of **1** instead of methyl ester) in methanol–dichloromethane–hexane (0.5:0.5:99) showed the presence of both monomer (λ_{max} = 648 nm) and aggregate species (λ_{max} = 738 nm). The RR spectrum of **1′** (Table 2) also gave two keto carbonyl peaks, 1701 and 1651 cm^{-1}. The former comes from the monomer and the latter comes from the aggregate. The latter value is similar to the value of C=O in the methanol-assisted complex of **7**. Therefore, the aggregate of **1′** also has the special hydrogen-bonding, C=O···H(X)O···Zn.

The zinc complex of 3^1-dimethylaminochlorin **8** (see Fig. 3) in dichloromethane was in the monomeric form from the visible spectral analysis [32]. When the dichloromethane solution was progressively diluted with cyclohexane, the 423 and 648 nm maxima of **8** decreased concomitant with the increase of new bands at 443 and 670 nm which grew to become the predominant peaks in dichloromethane–cyclohexane (1:99). Evidently, the non-polar solution contained at least two species,

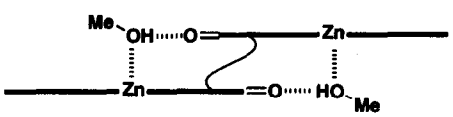

Fig. 4. Methanol-assisted locked "dimer".

the monomer **8** and a main species. By comparison with reported data of chlorin dimers [55–60], the new band can be ascribed to a dimeric structure of **8**.

Fig. 5 shows two possible arrangements for a dimer of **8**, I and II. Parallel dimer I (head-to-tail type) is ruled out for dimeric **8** by the observation that addition of the zinc chlorin **3** with an ethyl group at the 3-position to the dichloromethane–cyclohexane solution of **8** did not affect the 670 nm absorption band. Therefore, the anti-parallel arrangement (head-to-head type) II (M=Zn, L=$\underline{N}(CH_3)_2$ in Fig. 5) can be assigned to the dimer of **8**, which has been ascribed previously to a dimer of magnesium hydroxychlorins (M=Mg, L=$\underline{O}H$) on the basis of ^1H NMR evidence [50,61]. Under the same conditions, the visible spectra showed that the mixture of monomer and dimer was predominant in the non-polar organic solution of **10** as well as in **9** [32].

Zinc chlorin **1** with a hydroxyl group gave relatively large oligomers with a Q_y maximum at 740 nm and the absorption edge at >800 nm [30]. Zinc chlorin **8–10**, with an amino group, dimerized and did not aggregate to form any oligomers absorbing at around the 740 nm maximum. Only minor amounts of small aggregates with an absorption edge at <750 nm were observed in **9** and **10**, but the compound **8** (without a hydrogen-donating NH group) did not absorb in this region. The behavior of the hydroxychlorin **1** and the amino analogues **8–10** in the non-polar solvents was thus markedly different. The explanation that this difference in aggregation arises from a difference in hydrogen bonding between C=O···HO and C=O···HN can be ruled out by the observation that both primary alcohols and amines afforded the same Chl-*a* aggregates in non-polar organic solvents [62]. It appears rather more probable that dimer II and large oligomer formation have different bonding requirements.

The difference between aggregation of **1** and **10** may be explained as follows. The "intrabimolecular" coordination of the free amino group in the dimer I of **10** to the free Zn of the opposite molecule leads to highly stable dimer II, which could form small aggregates, most likely trimers and tetramers, by coordination with a monomer and second dimer, respectively. In contrast, the dimer II of hydroxychlorin–**1** (L=$\underline{O}H$) is expected to be less stable than the amino analog II (L=$\underline{N}H_2$) because coordination of Zn···O is weaker than that of Zn···N. Thus, the Zn···O bond in

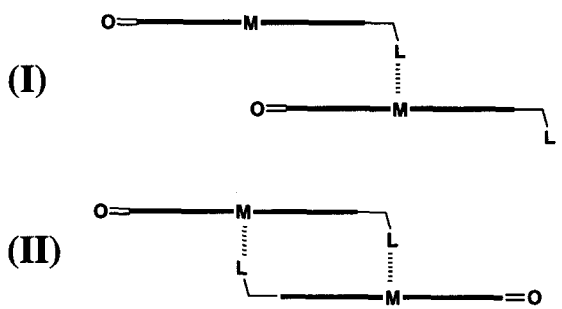

Fig. 5. Dimeric structures of metallochlorin; parallel head-to-tail (I) and anti-parallel head-to-head arrangements (II).

dimer II breaks to re-form dimer I, and the free zinc of the dimer I (L=OH) aggregates through coordination with the hydroxyl oxygen of a third molecule and hydrogen bonding C=O···H(X)O···Zn to form large oligomers.

From the above model studies, it is concluded that the dimer II represents a "dead end" species and dimer I should be an "active" dimer. The dimer I is reactive, and could hardly be detected, and thus easily aggregates to form an oligomer whose supramolecular structure is shown in Fig. 6 (postulated first by Worcester et al. [41]).

2.3. *In-vivo BChl-c aggregates*

The RR spectra of magnesium chlorins **11**–**13** (see Fig. 3) in non-polar organic solvents (methanol–dichloromethane–cyclohexane) were measured (see Table 2) [53]. The 1698 cm^{-1} band in **11** (0:1:99 plus 0.1% pyridine) in addition to visible maxima at 426 and 648 nm was assigned to the 13^1-keto carbonyl stretching vibration free from any intramolecular interaction. The 1646 cm^{-1} band in **12** (0.01:1:99) in addition to λ_{max}=431 and 679 nm was about 50 cm^{-1} down-shifted and clearly assignable to the carbonyl stretching vibration in C=O···H(Me)O···Mg, in comparison with the results of **7** with two zinc–chlorins in the molecule. The RR peak at 1642 cm^{-1} of hydroxychlorin Mg–**13** (0.2:0.8:99) with λ_{max}=454 and 755 nm indicated the presence of the special hydrogen-bonding in the aggregates of magnesium chlorins. The RR spectra of BChl-*c* in native chlorosomes gave the keto carbonyl vibration stretching around 1639–1645 cm^{-1} [13,63,64]. Lutz et al. [39,40] speculatively assigned this peak to direct interaction between keto carbonyl and magnesium, C=O···Mg. Our results clearly and directly show that this peak comes from C=O···H(X)O···Mg. Therefore, the BChl-*c* aggregates in chlorosomes have a similar special hydrogen-bonded structure to the above zinc chlorin aggregates. For the

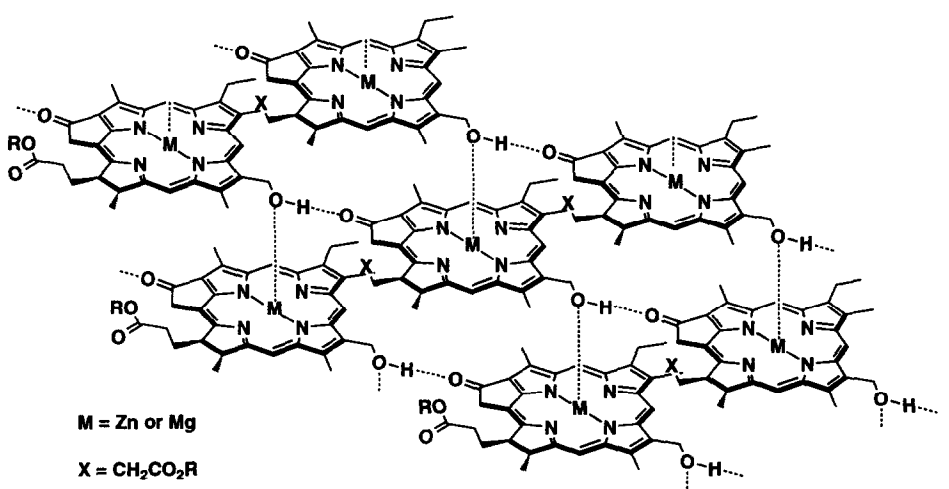

Fig. 6. Proposed supramolecular structure for self-aggregates of metallochlorin (adapted from Ref. [31]).

BChl-*c* aggregates, the arrangements depicted by models (A), (B) and (C) are ruled out and models (D), (E) and (F) remain.

The similarity of the visible, CD, RR and IR spectra of the in-vitro aggregates of zinc and magnesium chlorins to those of the in-vivo aggregates in chlorosome [31] shows that the supramolecular structures in artificial and natural aggregates of magnesium chlorins should be similar to those of zinc chlorin aggregates. The natural aggregates of BChls-*c* and *d* in the chlorosome should take model (D) of Fig. 2 and the supramolecular structure is shown in Fig. 6.

Matsuura et al. [65] measured CD and LD spectra of in-vivo aggregates and proposed model (E) where the anti-parallel chains make the surface of a chlorosomal rod and the hydrocarbon chains of the ester form the hydrophobic core interior of the rod. Nozawa et al. [49] proposed BChl-*c* aggregates with stacking of the anti-parallel chain planes (as model (E), vide supra) perpendicular to a rod surface and the hydrocarbon chains of the ester both inside and outside the rod.

Recently, Holzwarth et al. [66] calculated the energy in aggregates of a BChl-*d* derivative by use of molecular mechanics and found the optimized supramolecular structure. In the most stable supramolecular structure, a two-dimensional sheet formed by model (D) (see also Fig. 6) covered the surface of a cylindrical rod. They showed that the hydrocarbon chains of the ester should be located out of the rod in the chlorosomes. In natural chlorosome, substituents at the 8-position affected the diameter of the rod [1] and visible absorption bands [67]. These effects were easily explained in the estimated supramolecular structures. These calculated results concretely support the supramolecular structures supposed from experimental results by Worcester's [41,43] and our groups [19,30–32,53,68].

In conclusion, elucidation of the supramolecular structures as shown in Fig. 6 indicated that chlorosomal pigments are formed by the self-aggregation of BChl-*c*. Some polypeptides (5.7, 11 and 18 kDa for *Chloroflexus aurantiacus*) obtained from extracted chlorosomes are located in the lipid monolayer of the chlorosome and outside the rod elements [69,70] and clearly play no important role in the construction of the in-vivo aggregates, whereas the polypeptides present in other antennae interact with the pigments to form light-harvesting complexes.

Acknowledgements

The author gratefully acknowledges collaboration with Prof. Dr. Kurt Schaffner, Dr. Alfred R. Holzwarth, Dr. Peter Hildebrandt, Dr. Silviu T. Balaban, Dr. Kai Griebenow, Mr. Michael Reus (Max-Planck-Institut für Strahlenchemie, Mülheim an der Ruhr, Germany) and Prof. Dr. Rikuhei Tanikaga, Mr. Masaaki Amakawa, Mr. Takayuki Kubota, Mr. Yasuhiko Kureishi, Mr. Shoichiro Takeuchi, Mr. Shinya Miyata, Mr. Hiroyasu Ichikawa, Mr. Naoya Umezaki, Mr. Yoshiyuki Shimono, Ms. Satoko Nagano, Ms. Kaoru Matsushita, Mr. Tomohiro Miyatake, Dr. Alistair G.M. Rattray (Ritsumeikan University). This work was partially supported by Grants-in-Aid for Scientific Research (No. 05808052 and 06808057) from the Ministry of Education, Science and Culture (Japan), the Mazda Foundation's Research Grant,

the Japan Securities Scholarship Foundation, Research Foundation for Material Science, Yazaki Memorial Foundation for Science and Technology, Nissan Science Foundation, and Ritsumeikan University Foundation Memorial Trust Research Fund. The author also thanks the Alexander-von-Humboldt Foundation and Max-Planck-Society for a post-doctoral fellowship.

References

[1] J.M. Olson, Biochim. Biophys. Acta, 594 (1980) 33.
[2] H. Zuber and R.A. Brunisholz, in S. Hugo (ed.), Chlorophylls, CRC, Boca Raton, FL, 1991, p. 627.
[3] S.C.M. Otte, J.C. van der Heiden, N. Pfenning and J. Amesz, Photosynth. Res., 28 (1991) 77.
[4] K.M. Smith, Photosynth. Res., 41 (1994) 23.
[5] F. Fages, N. Griebenow, K. Griebenow, A.R. Holzwarth and K. Schaffner, J. Chem. Soc., Perkin Trans. 1, (1990) 2791.
[6] T. Wechsler, F. Suter, R.C. Fuller and H. Zuber, FEBS Lett., 181 (1985) 173.
[7] M.I. Bystrova, I.N. Mal'gosheva and A.A. Krasnovskii, Mol. Biol., 13 (1979) 440.
[8] K. Griebenow and A.R. Holzwarth, Biochim. Biophys. Acta, 973 (1989) 235.
[9] A.R. Holzwarth, K. Griebenow and K. Schaffner, Z. Naturforsch., 45c (1990) 203.
[10] K. Griebenow, A.R. Holzwarth and K. Schaffner, Z. Naturforsch., 45c (1990) 823.
[11] K. Griebenow and A.R. Holzwarth, in G. Drews and E.A. Dawes (eds.), Molecular Biology of Membrane-Bound Complexes in Phototropic Bacteria, Plenum, New York, 1990, p. 375.
[12] K. Griebenow, A.R. Holzwarth, F. van Mourik and R. van Grondelle, Biochim. Biophys. Acta, 1058 (1991) 194.
[13] P. Hildebrandt, K. Griebenow, A.R. Holzwarth and K. Schaffner, Z. Naturforsch., 46c (1991) 228.
[14] K. Schaffner, S.E. Braslavsky and A.R. Holzwarth, in H.-J. Schneider and H. Dürr (Eds.), Frontiers in Supramolecular Organic Chemistry and Photochemistry, VCH, Weinheim, 1991, p. 421.
[15] A.R. Holzwarth, K. Griebenow and K. Schaffner, Photochem. Photobiol. A: Chem., 65 (1992) 61.
[16] M. Hirota, T. Moriyama, K. Shimada, M. Miller, J.M. Olson and K. Matsuura, Biochim. Biophys. Acta, 1099 (1992) 271.
[17] M. Miller, T. Gillbro and J.M. Olson, Photochem. Photobiol., 57 (1993) 98.
[18] K. Uehara, M. Mimuro, Y. Ozaki and J.M. Olson, Photosynth. Res., 41 (1994) 235.
[19] H. Tamiaki, A.R. Holzwarth and K. Schaffner, 8th European Bioenergetics Conference, Valencia, Spain, Sep. 12–17, 1994, Elsevier, Amsterdam, p. 72.
[20] G. Niedermeier, H. Scheer and R.G. Feick, Eur. J. Biochem., 204 (1992) 685.
[21] R.P. Lehmann, R.A. Brunisholz and H. Zuber, FEBS Lett., 342 (1994) 319.
[22] R.P. Lehmann, R.A. Brunisholz and H. Zuber, Photosynth. Res., 41 (1994) 165.
[23] M. Mimuro, T. Nozawa, N. Tamai, K. Shimada, I. Yamazaki, S. Lin, R.S. Knox, B.P. Wittmershaus, D.C. Brune and R.E. Blankenship, J. Phys. Chem., 93 (1989) 7503.
[24] A.R. Holzwarth, M.G. Müller and K. Griebenow, J. Photochem. Photobiol. B: Biol., 5 (1990) 457.
[25] M.G. Müller, K. Griebenow and A.R. Holzwarth, Biochim. Biophys. Acta, 1144 (1993) 161.
[26] S. Savikhin, Y. Zhu, S. Lin, R.E. Blankenship and W.S. Struve, J. Phys. Chem., 98 (1994) 10322.
[27] M. Mimuro, M. Hirota, Y. Nishimura, T. Moriyama, I. Yamazaki, K. Shimada and K. Matsuura, Photosynth. Res., 41 (1994) 181.
[28] P.I. van Noort, C. Francke, N. Schoumans, S.C.M. Otte, T.J. Aartsma and J. Amesz, Photosynth. Res., 41 (1994) 193.
[29] J. Pšenčík, M. Vácha, F. Adamec, M. Ambrož, J. Dian, J. Boček and J. Hála, Photosynth. Res., 42 (1994) 1.
[30] H. Tamiaki, A.R. Holzwarth and K. Schaffner, J. Photochem. Photobiol. B: Biol., 15 (1992) 355.
[31] H. Tamiaki, M. Amakawa, Y. Shimono, R. Tanikaga, A.R. Holzwarth and K. Schaffner, Photochem. Photobiol., 63 (1996).
[32] H. Tamiaki, A.R. Holzwarth and K. Schaffner, Photosynth. Res., 41 (1994) 245.

[33] H. Scheer, J.J. Katz and J.R. Norris, J. Am. Chem. Soc., 99 (1977) 1372.
[34] K. Ballschmiter and J.J. Katz, J. Am. Chem. Soc., 91 (1969) 2661.
[35] J.M. Olson, P.D. Gerola, G.H. van Brakel, R.F. Meiburg and H. Vasmel, in M.E. Michel-Bayerle (Ed.), Antennas and Reaction Centers of Photosynthetic Bacteria, Springer-Verlag, Berlin, 1985, p. 67.
[36] D.C. Brune, T. Nozawa and R.E. Blankenship, Biochemistry, 26 (1987) 8644.
[37] R.E. Blankenship, D.C. Brune, J.M. Freeman, G.H. King, J.H. McManus, T. Nozawa, J.T. Trost and B.P. Wittmershaus, in J.M. Olson, J.G. Ormerod, J. Amesz, E. Stackebrandt and H.G. Trüper (Eds.), Green Photosynthetic Bacteria, Plenum Press, New York, 1988, p. 57.
[38] K.M. Smith, L.A. Kehres and J. Fajer, J. Am. Chem. Soc., 105 (1983) 1387.
[39] M. Lutz and G. van Brakel, in J.M. Olson, J.G. Ormerod, J. Amesz, E. Stackebrandt and H.G. Trüper (Eds.), Green Photosynthetic Bacteria, Plenum, New York, 1988, p. 23.
[40] M. Lutz and W. Mäntele, in S. Hugo (Ed.), Chlorophylls, CRC, Boca Raton, FL, 1991, p. 855.
[41] D.L. Worcester, T.J. Michalski and J.J. Katz, Proc. Natl. Acad. Sci. USA, 83 (1986) 3791.
[42] D.C. Brune, G.H. King and R.E. Blankenship, in H. Scheer and S. Schneider (Eds.), Photosynthetic Light-Harvesting Systems, Walter de Gruyter, Berlin, 1988, p. 141.
[43] J.J. Katz, M.K. Bowman, T.J. Michalski and D.L. Worcester, in S. Hugo (Ed.), Chlorophylls, CRC, Boca Raton, FL, 1991, p. 211.
[44] K. Uehara, Y. Ozaki, K. Okada and J.M. Olson, Chem. Lett., (1991) 909.
[45] K. Uehara and J.M. Olson, Photosynth. Res., 33 (1992) 251.
[46] R.G. Alden, S.H. Lin and R.E. Blankenship, J. Luminesc., 51 (1992) 51.
[47] T. Nozawa, M. Suzuki, S. Kanno and S. Shirai, Chem. Lett., (1990) 1805.
[48] T. Nozawa, M. Suzuki, K. Ohtomo, Y. Morishita, H. Konami and M.T. Madigan, Chem. Lett., (1991) 1641.
[49] T. Nozawa, K. Ohtomo, M. Suzuki, H. Nakagawa, Y. Shikama, H. Konami and Z.-Y. Wang, Photosynth. Res., 41 (1994) 211.
[50] T. Nozawa, K. Ohtomo, Y. Morishita, H. Konami and M.T. Madigan, Chem. Lett., (1992) 261.
[51] T. Nozawa, K. Ohtomo, M. Suzuki, M. Morishita and M.T. Madigan, Bull. Chem. Soc. Jpn., 66 (1993) 231.
[52] W.R. Scheidt, M.E. Kastner and K. Hatano, Inorg. Chem., 17 (1978) 706.
[53] P. Hildebrandt, H. Tamiaki, A.R. Holzwarth and K. Schaffner, J. Phys. Chem., 98 (1994) 2192.
[54] S.G. Boxer and G.L. Closs, J. Am. Chem. Soc., 98 (1976) 5406.
[55] J.M. Olson and J.P. Pederson, in H. Scheer and S. Schneider (Eds.), Photosynthetic Light-Harvesting Systems, Walter de Gruyter, Berlin, 1988, p. 365.
[56] J.M. Olson, J.P. Pederson, T.P. Causgrove, D.C. Brune and R.E. Blankenship, in M. Baltscheffsky (Ed.), Current Research in Photosynthesis, Vol. II, Kluwer, Netherlands, 1990, p. 37.
[57] T.P. Causgrove, D.C. Brine, R.E. Blankenship and J.M. Olson, Photosynth. Res., 25 (1990) 1.
[58] J.M. Olson and J.P. Pedersen, Photosynth. Res., 25 (1990) 25.
[59] J.M. Olson and R.P. Cox, Photosynth. Res., 30 (1991) 35.
[60] J.M. Olson, Photosynth. Res., 30, (1991) 45.
[61] K.M. Smith, F.W. Bobe, D.A. Goff and R.J. Abraham, J. Am. Chem. Soc., 108 (1986) 1111.
[62] T.M. Cotton, P.A. Loach, J.J. Katz and K. Ballschmiter, Photochem. Photobiol., 27 (1978) 735.
[63] T. Nozawa, T. Noguchi and M. Tasumi, J. Biochem., 108 (1990) 737.
[64] U. Feiler, D. Albouy, M. Lutz and B. Robert, Photosynth. Res., 41 (1994) 175.
[65] K. Matsuura, M. Hirota, K. Shimada and M. Mimuro, Photochem. Photobiol., 57 (1993) 92.
[66] A.R. Holzwarth and K. Schaffner, Photosynth. Res., 41 (1994) 225.
[67] F.W. Bobe, N. Pfenning, K.L. Swanson and K.M. Smith, Biochemistry, 29 (1990) 4340.
[68] H. Tamiaki, S. Takeuchi, R. Tanikaga, S.T. Balaban, A.R. Holzwarth and K. Schaffner, Chem. Lett., (1994) 401.
[69] W. Wullink, J. Knudsen, J.M. Olson, T.E. Redlinger and E.F.J. van Bruggen, Biochim. Biophys. Acta, 1060 (1991) 97.
[70] M. Foidl, J.R. Golecki and J. Oelze, Photosynth. Res., 41 (1994) 145.